Effect of Multiple Grooves on Aerodynamic Performance of a Low Reynolds Number UAV Propeller (Part I)

Aravind SEENI*

*Corresponding author
Department of Aeronautical Engineering, Rajalakshmi Engineering College,
Thandalam, Chennai 602 105, India,
aravindseeni.s@rajalakshmi.edu.in

DOI: 10.13111/2066-8201.2023.15.2.9

Received: 07 July 2022/ Accepted: 21 March 2023/ Published: June 2023

Abstract: *In a continuation of work previously performed by the author on grooved propellers, numerical investigations are performed on Applied Precision Composites 10×7 Slow Flyer propeller. Computational Fluid Dynamics is used to analyze the novel propeller design. The grooved sections considered have a rectangular geometry measuring 0.1×0.1mm and are interchangeably located at 0.09c, 0.17c, 0.32c and 0.42c from the leading edge in a dual grooved configuration. The results of the study showed that the presence of grooves had modified the flow characteristics only to detrimentally impact the thrust performance. However, the grooves improved power performance due to torque reduction. The analysis of the results showed that, for most models, there is lower torque relative to the baseline in the low-to-medium advance ratio operating range. The improvement in torque however, did not improve efficiency in the models.*

Key Words: *passive flow control, grooved propeller, aerodynamic performance, UAV range, UAV endurance*

1. INTRODUCTION

The research described in this paper is an extension of the earlier work by the same author [1], [2]. In the earlier published research, 17 models namely, Model − 1 to Model – 17, are analysed and the performance and efficiency results reported. In this paper, the focus is on the results obtained for 6 additional models.

Research on improving the efficiency of UAV propellers helps to increase and adds value to future applications of drones. The desired design requirement is a propelling device capable of producing improved thrust and reduced torque at a low Re. Modern research is concerned with improving the thrust through flow modifiers or flow control technique.

These flow modifiers alter the fluid flow such that the flow trajectory is optimized around the aerodynamic body to attain the desired performance. The current research is concerned with studying the flow control technique called grooved design. In the present work, a comprehensive study on grooved propeller design has been performed with the aim to study its significance for the aeronautical application. The unique features of an aeronautical propeller are low torque, high thrust and high efficiency during operation. The effect of positioning the grooves in multiple locations on the performance characteristics of the propeller will be investigated. The positioning of multiple grooves could have either favorable

or detrimental impact on the aerodynamic performance. These have not been investigated so far and will be investigated in the current work.

2. METHODOLOGY

As in the case of earlier papers, Computational Fluid Dynamics is used to solve the governing equations of fluid flow. RANS simulations are performed with different propeller models as a first step of initiating the research on fluid dynamic analysis of grooved propeller.

2.1 Baseline propeller

Applied Precision Composites (APC) 10×7 *Slow Flyer (SF)* is considered as the baseline propeller in this study. APC10x7SF is widely used in low *Re*applications such as small-scale UAVs. This propeller is chosen based on the availability of data from the experiments of Brandt *et al.* [3].The propeller has a diameter (*D*) of 0.254 m and pitch of 0.1778 m. Low *Re* Eppler E63 air foil sections near the hub and thin Clark-Y air foil sections near the tip are used to design the propeller. For the simulation, the propeller is assumed to be rotating at a constant rotational speed of 3008 rpm.

2.2 Grooved propellers

The design of propellers is performed using CAD software Catia v5. For the design of grooved propeller, baseline propeller model is modified with grooves of varying dimensions. To study the effect of multiple grooves, 0.1mm × 0.1mm grooves are placed interchangeably at different positions, namely 0.09*c*, 0.17*c*, 0.32*c* and, 0.42*c*. The dimensions of the grooves are varied for different positions, as listed in Table 1.

Table 1 – Propeller configurations to study the effect of dual grooves

Name	Groove size, mm	Groove position, x_{LE}
Model−18	0.1mm × 0.1mm	0.09*c*, 0.17*c*
Model−19	0.1mm × 0.1mm	0.09*c*, 0.32*c*
Model−20	0.1mm × 0.1mm	0.09*c*, 0.42*c*
Model−21	0.1mm × 0.1mm	0.17*c*, 0.32*c*
Model−22	0.1mm × 0.1mm	0.17*c*, 0.42*c*
Model−23	0.1mm × 0.1mm	0.32*c*, 0.42*c*

3. RESULTS AND DISCUSSIONS

3.1 Verification and validation

The verification and validation of the model for the baseline propeller is provided in Seeni [1].

3.2 Effect of multiple grooves on propeller performance

3.2.1 Model−18

The performance results of Model−18 grooved design are provided in Table 2. Model−18 multi-grooved design showed decreased K_T for 12 cases of *J*, 0.192 to 0.717. The difference varied between −4.01% and −14.18% for those *J*. For higher *J* of 0.773 and 0.799, higher K_T compared to baseline was produced. The difference varied as much as 9.58% and 28.49% for

those J, respectively. K_P for this grooved design showed decrement for J between 0.192 and 0.527. The difference varied between −1.04% and −5.45%. However, for higher J from 0.573 to 0.799, the K_P increased relative to the baseline design. The η for this grooved design remained lower relative for a baseline for most J from 0.192 to 0.773. Only for J of 0.799, the η was found to be higher compared to the baseline design.

Table 2 – Performance and efficiency results of Model−18

Case	Condition J	K_T	ΔK_T [%]	$10K_P$	ΔK_P [%]	η [%]	$\Delta\eta$ [%]
1	0.192	0.1079	−14.18	0.6439	−5.45	32.17	−9.39
2	0.236	0.1039	−12.05	0.6364	−3.86	38.52	−8.51
3	0.282	0.0993	−10.48	0.6265	−3.01	44.68	−7.68
4	0.334	0.0930	−9.49	0.6111	−2.84	50.80	−6.95
5	0.383	0.0858	−9.72	0.5920	−2.95	55.49	−6.90
6	0.432	0.0786	−9.19	0.5702	−2.69	59.51	−6.87
7	0.486	0.0709	−7.44	0.5454	−1.38	63.18	−6.26
8	0.527	0.0640	−7.58	0.5205	−1.04	64.75	−6.70
9	0.573	0.0564	−7.04	0.4922	0.04	65.69	−7.21
10	0.628	0.0458	−7.08	0.4517	1.74	63.68	−8.63
11	0.659	0.0394	−7.47	0.4256	2.06	61.04	−9.44
12	0.717	0.0278	−4.01	0.3750	5.64	53.22	−9.18
13	0.773	0.0157	9.58	0.3211	13.45	37.73	−3.51
14	0.799	0.0100	28.49	0.2938	16.60	27.25	10.33

The three-dimensional velocity distribution of the fluid surrounding the Model−18 grooved propeller is modified or reduced to detrimentally affect thrust. The velocity distribution along a plane bisecting the flow field along y-z for two J case samples, 0.334 and 0.573 is shown in Fig. 1. For the J=0.334 case, the peak velocity is reduced compared to baseline. For J=0.573, the peak velocity is maintained closely similar to the baseline model.

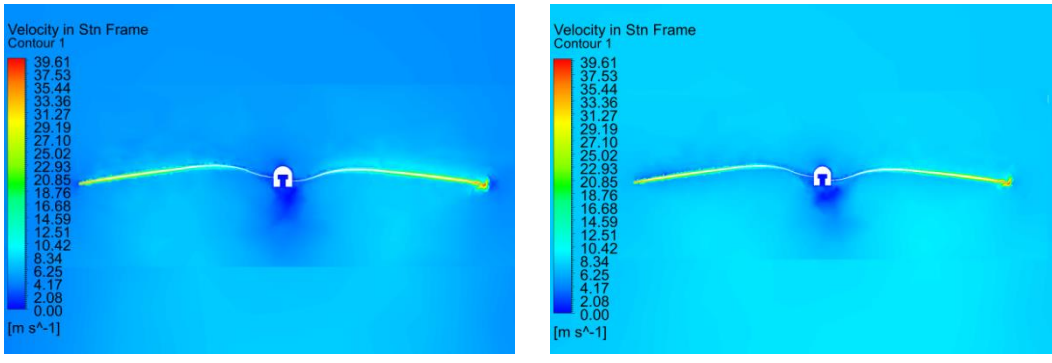

(a) (b)

Fig. 1 – Velocity flow-field around Model−18 propeller for (a) J=0.334 and (b) J=0.573

The velocity modifications in the presence of the groove modifies the pressure distribution to affect the thrust. Lower peak pressures are maintained on the pressure side (aft) as compared to baseline whereas higher low pressures are maintained on the suction side (fore) as compared to baseline for both J=0.334. For J=0.573 case, higher peak pressures are maintained on the pressure side (aft) as compared to baseline whereas lower low pressures are maintained on the suction side (fore) as compared to baseline. Fig. 2 shows the modified pressure levels on the

pressure side and on the suction side in the presence of groove for two *J* cases, 0.334 and 0.573 when viewed along the y-z plane bisecting the flow field.

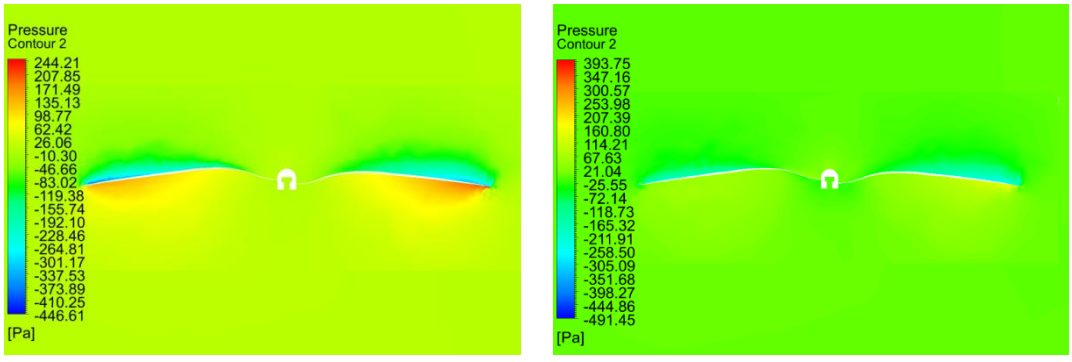

(a) (b)

Fig. 2 – Pressure contour of flow around Model−18 propeller for (a) *J*=0.334 and (b) *J*=0.573

Vector plots of fluid flow at 0.75R radial distance and velocity distribution for three-dimensional Model−18 propeller is provided in Fig. 3 for single *J* condition *J*=0.334 to illustrate that the velocity very near to the blade surface is modified in the presence of groove.

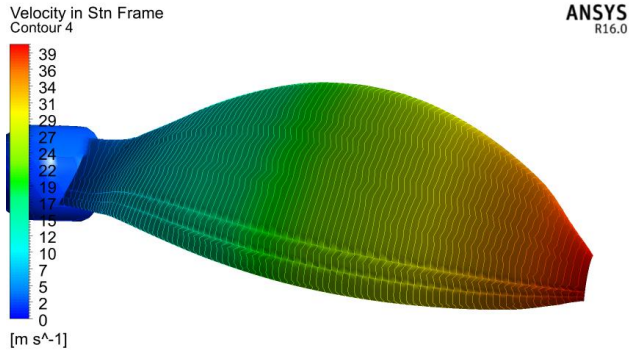

Fig. 3 – Velocity distribution on Model−18 propeller blade for *J*=0.334

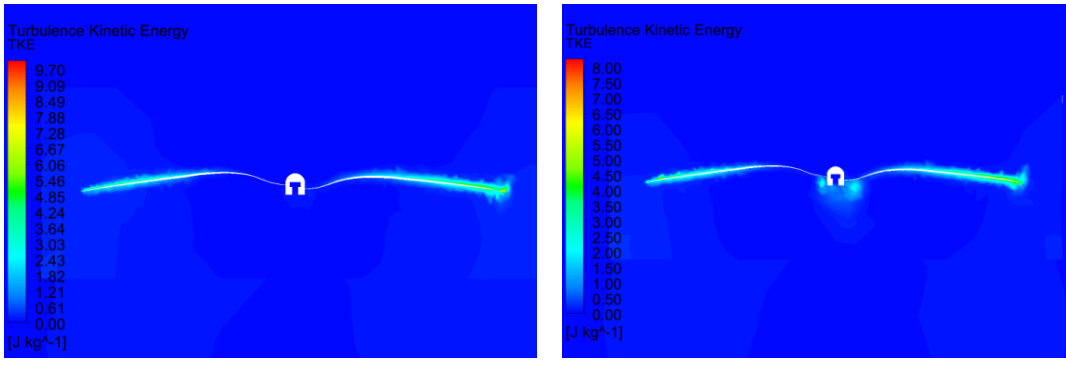

(a) (b)

Fig. 4 – Turbulence Kinetic Energy of Model−18 propeller for (a) *J*=0.334 and (b) *J*=0.573

A measure of turbulence can be provided through Turbulence Kinetic Energy (TKE) which is a turbulence quantity. Model−18 grooved design has increased TKE along the blade radii compared to baseline for J=0.334 (Fig. 4(a)). For J=0.573, the TKE is decreased (Fig. 4(b)).

3.2.2 Model−19

The performance and efficiency results of Model−19 grooved design are provided in Table 3. The relative difference between the results with baseline propeller is also listed in the table.

Table 3 – Performance and efficiency results of Model−19

Case	Condition J	K_T	ΔK_T [%]	$10K_P$	ΔK_P [%]	η [%]	$\Delta\eta$ [%]
1	0.192	0.1034	−17.76	0.6029	−11.46	32.92	−7.27
2	0.236	0.0998	−15.47	0.5984	−9.60	39.37	−6.49
3	0.282	0.0948	−14.52	0.5873	−9.08	45.52	−5.96
4	0.334	0.0886	−13.73	0.5735	−8.82	51.60	−5.50
5	0.383	0.0823	−13.41	0.5584	−8.45	56.42	−5.34
6	0.432	0.0754	−12.86	0.5397	−7.89	60.33	−5.59
7	0.486	0.0674	−12.00	0.5136	−7.13	63.79	−5.36
8	0.527	0.0602	−12.94	0.4889	−7.06	64.95	−6.42
9	0.573	0.0520	−14.37	0.4592	−6.66	64.85	−8.40
10	0.628	0.0419	−15.06	0.4205	−5.30	62.54	−10.27
11	0.659	0.0357	−16.27	0.3944	−5.41	59.60	−11.58
12	0.717	0.0243	−16.12	0.3468	−2.32	50.30	−14.17
13	0.773	0.0124	−12.95	0.2959	4.56	32.52	−16.84
14	0.799	0.0067	−14.24	0.2706	7.39	19.75	−20.04

Model−19 multi-grooved design produced K_T lower for all J cases chosen for this study. The decrement ranged between −12.00% and −17.76%. K_P, however, was lower for J from 0.192 to 0.717. The decrement ranged between −2.32% and −11.46%, respectively for those range of J. For J of 0.773 and 0.799, and the K_P was relatively higher compared to baseline. The difference lied at 4.56% and 7.39%. The η was found to relatively low for all J. The η difference varied between −5.34% and −20.04% ,respectively for those J relative to baseline.

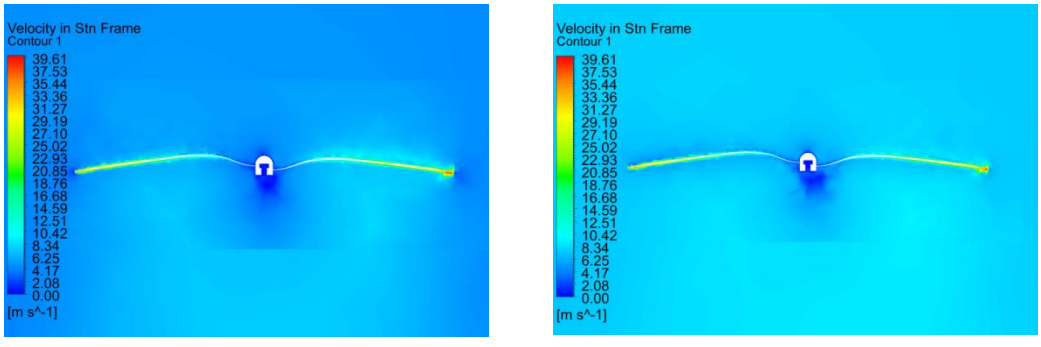

(a) (b)

Fig. 5 – Velocity flow-field around Model−19 propeller for (a) J=0.334 and (b) J=0.573

The three-dimensional velocity distribution of the fluid surrounding the Model−19 grooved propeller is modified or reduced to detrimentally affect thrust. The velocity

distribution along a plane bisecting the flow field along y-z for two *J* case samples, 0.334 and 0.573 is shown in Fig. 5.

It shows that for *J*=0.334, the peak velocities are modified and reduced compared to baseline. For *J*=0.573, the peak velocity remains closely similar as compared to baseline model with a velocity of 39.61 m/s.

The velocity modifications in the presence of the groove modifies the pressure distribution to affect the thrust. Lower peak pressures are maintained on the pressure side (aft) as compared to baseline whereas higher low pressures are maintained on the suction side (fore) as compared to baseline for both *J*=0.334 and *J*=0.573 cases.

Fig. 6 shows the modified pressure levels on the pressure side and on the suction side in the presence of groove for two *J* cases, 0.334 and 0.573 when viewed along the y-z plane bisecting the flow field.

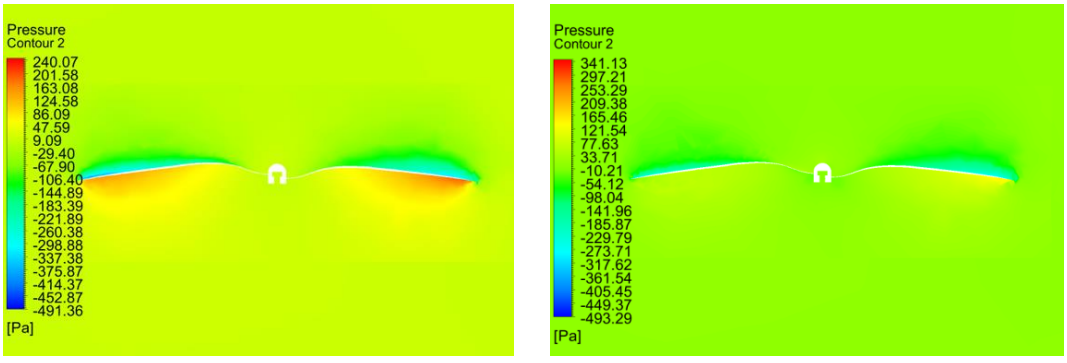

(a) (b)

Fig. 6 – Pressure contour of flow around Model−19 propeller for (a) *J*=0.334 and (b) *J*=0.573

Vector plots of fluid flow at 0.75R radial distance and velocity distribution for three-dimensional Model−19 propeller is provided in Fig. 7 for single *J* condition *J*=0.334 to illustrate that the velocity very near to the blade surface is modified in the presence of groove.

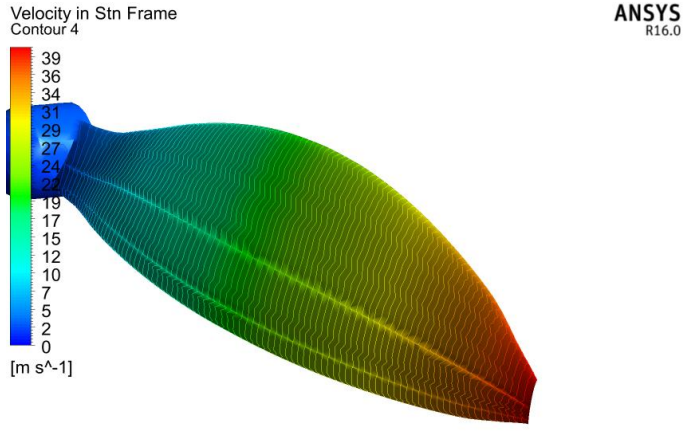

Fig. 7 – Velocity distribution on Model−19 propeller blade for *J*=0.334

A measure of turbulence can be provided through TKE which is a turbulence quantity. Model−19 grooved design has increased TKE along the blade radii compared to baseline for *J*=0.334 (Fig. 8(a)). For *J*=0.573, the TKE is decreased (Fig. 8(b)).

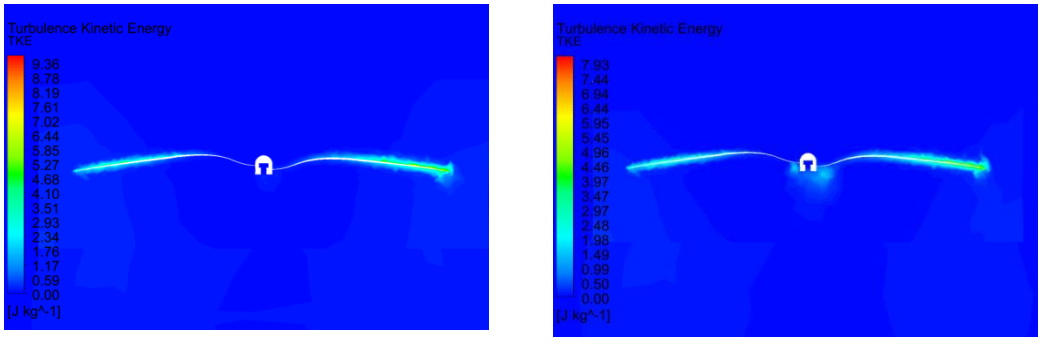

(a) (b)

Fig. 8 – Turbulence Kinetic Energy of Model 19 propeller for (a) J=0.334 and (b) J=0.573

3.2.3 Model−20

The performance and efficiency results of Model − 20 grooved design are provided in Table 4. The relative difference between the results with baseline propeller is also listed in the table.

For Model − 20 multi-grooved design, the relative difference of K_T varied between −5.70% and −13.01% for J ranging from 0.192 to 0.717. For higher J 0.773 and 0.799, K_T improved relative to baseline with the relative difference at 13.13% and 10.06%, respectively. K_P meanwhile decreased for J of 0.192 to 0.628. At higher J 0.659 to 0.799, the K_P improved relative to baseline contributing to reduced η. The η for this design decreased. for all cases of J analyzed relative to the baseline design. The η reduction ranged between −0.09% to a maximum of −11.19% for the J analyzed.

The three-dimensional velocity distribution of the fluid surrounding the Model−20 grooved propeller is modified or reduced to detrimentally affect thrust. The velocity distribution along a plane bisecting the flow field along y-z for two J case samples, 0.334 and 0.573 is shown in Fig. 9. For J=0.334, the peak velocity is reduced compared to baseline. For J=0.573, the peak velocity remains closely similar to baseline model.

Table 4 – Performance and efficiency results of Model−20

Case	Condition J	K_T	ΔK_T [%]	$10K_P$	ΔK_P [%]	η [%]	$\Delta\eta$ [%]
1	0.192	0.1094	−13.01	0.6459	−5.15	32.51	−8.44
2	0.236	0.1042	−11.74	0.6363	−3.88	38.66	−8.17
3	0.282	0.1006	−9.25	0.6285	−2.71	45.15	−6.71
4	0.334	0.0931	−9.39	0.6099	−3.04	50.96	−6.67
5	0.383	0.0886	−6.71	0.5996	−1.70	56.61	−5.02
6	0.432	0.0812	−6.12	0.5794	−1.13	60.55	−5.24
7	0.486	0.0722	−5.70	0.5478	−0.95	64.09	−4.91
8	0.527	0.0652	−5.85	0.5239	−0.41	65.54	−5.56
9	0.573	0.0550	−9.42	0.4854	−1.35	64.91	−8.32
10	0.628	0.0443	−10.17	0.4417	−0.53	62.97	−9.66
11	0.659	0.0389	−8.69	0.4219	1.18	60.75	−9.86
12	0.717	0.0267	−7.99	0.3676	3.55	52.04	−11.19
13	0.773	0.0162	13.13	0.3201	13.12	39.06	−0.09
14	0.799	0.0086	10.06	0.2846	12.95	24.10	−2.44

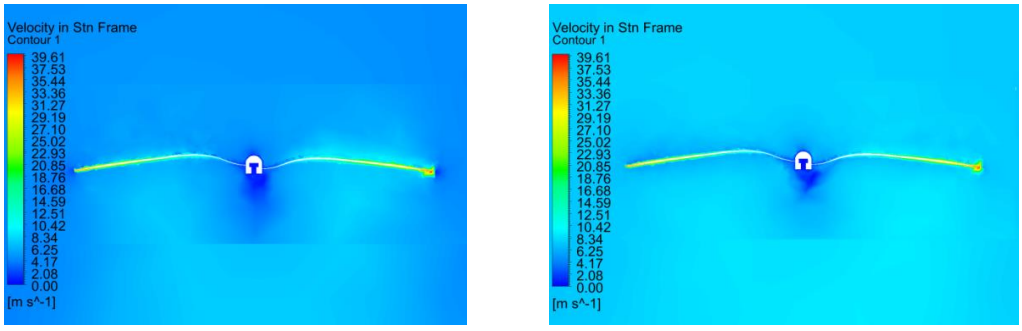

(a) (b)

Fig. 9 – Velocity flow-field around Model − 20 propeller for (a) *J*=0.334 and (b) *J*=0.573

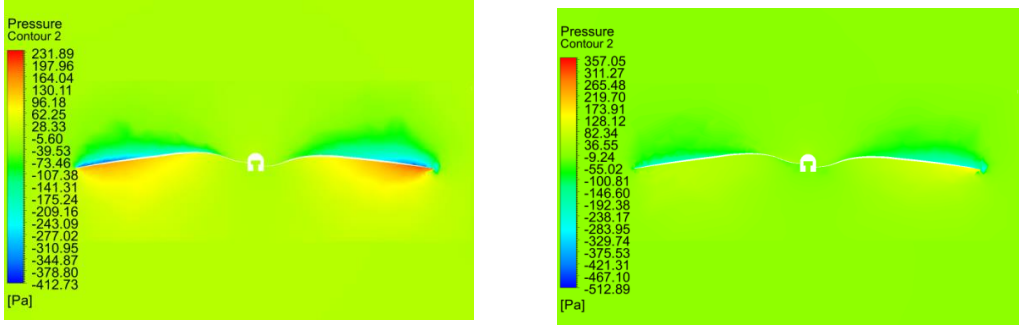

(a) (b)

Fig. 10 – Pressure contour of flow around Model − 20 propeller for (a) *J*=0.334 and (b) *J*=0.573

The velocity modifications in the presence of the groove modifies the pressure distribution to affect the thrust. Lower peak pressures are maintained on the pressure side (aft) as compared to baseline whereas higher low pressures are maintained on the suction side (fore) as compared to baseline for both *J*=0.334 and *J*=0.573 cases. Fig. 10 shows the modified pressure levels on the pressure side and on the suction side in the presence of groove for two *J* cases, 0.334 and 0.573 when viewed along the y-z plane bisecting the flow field. Vector plots of fluid flow at 0.75R radial distance and velocity distribution for three-dimensional Model−20 propeller is provided in Fig. 11 for single *J* condition *J*=0.334 to illustrate that the velocity very near to the blade surface is modified in the presence of groove. A measure of turbulence can be provided through TKE which is a turbulence quantity. Model − 20 grooved design has increased TKE along the blade radii compared to baseline for *J*=0.334 and *J*=0.573 (Fig. 12).

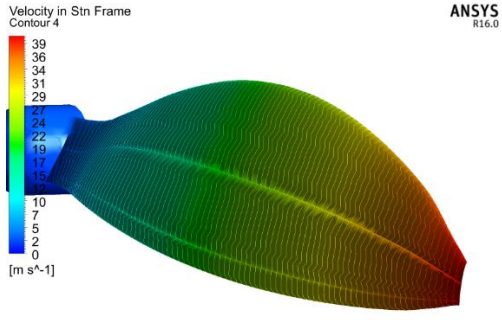

Fig. 11 – Velocity distribution on Model−20 propeller blade for *J*=0.334

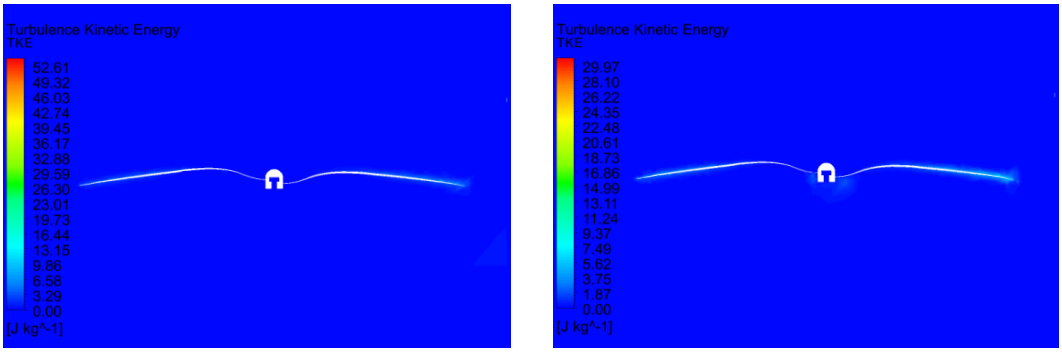

(a) (b)

Fig. 12 – Turbulence Kinetic Energy of Model − 20 propeller for (a) J=0.334 and (b) J=0.573

3.2.4 Model−21

The performance and efficiency results of Model − 21 grooved design are provided in Table 5. Model − 21 produced reduced thrust for J from 0.192 to 0.334. From J of 0.383, K_T increased relative to baseline.

K_P also increased relative to baseline for all J analyzed. The increment was found in the range of 2.24% to 34.60%. The η, when compared to baseline, was found to be reduced for J of 0.192 to 0.717.

For J 0.773 and 0.799, the η was found to be increased. The three-dimensional velocity distribution of the fluid surrounding the Model−21 grooved propeller is modified or reduced to detrimentally affect thrust.

The velocity distribution along a plane bisecting the flow field along y-z for two J case samples, 0.334 and 0.573 is shown in Fig. 13.

The results show that for J=0.334, the peak velocity is reduced whereas for J=0.573, the peak velocity is increased compared to baseline.

Table 5 – Performance and efficiency results of Model−21

Case	Condition J	K_T	ΔK_T [%]	$10K_P$	ΔK_P [%]	η [%]	$\Delta\eta$ [%]
1	0.192	0.1162	−7.53	0.7797	14.50	28.62	−19.37
2	0.236	0.1123	−4.91	0.6768	2.24	39.16	−6.98
3	0.282	0.1076	−2.97	0.6716	3.96	45.18	−6.64
4	0.334	0.1017	−0.97	0.6634	5.46	51.21	−6.22
5	0.383	0.0955	0.49	0.6521	6.91	56.07	−5.93
6	0.432	0.0882	1.98	0.6339	8.17	60.12	−5.92
7	0.486	0.0797	4.08	0.6104	10.38	63.48	−5.82
8	0.527	0.0726	4.98	0.5877	11.73	65.14	−6.14
9	0.573	0.0641	5.68	0.5574	13.29	65.94	−6.86
10	0.628	0.0532	8.01	0.5148	15.94	64.96	−6.80
11	0.659	0.0467	9.53	0.4869	16.75	63.16	−6.30
12	0.717	0.0338	16.46	0.4310	21.42	56.18	−4.13
13	0.773	0.0207	44.53	0.3712	31.17	43.04	10.07
14	0.799	0.0138	77.56	0.3392	34.60	32.62	32.08

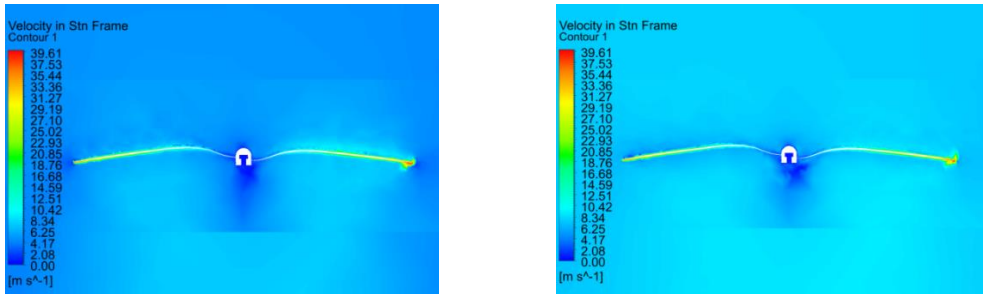

(a) (b)

Fig. 13 – Velocity flow-field around Model − 21 propeller for (a) *J*=0.334 and (b) *J*=0.573

Model−21 produced reduced thrust for *J* from 0.192 to 0.334. From *J* of 0.383, K_T increased relative to baseline. K_P also increased relative to baseline for all *J* analyzed. The increment was found in the range of 2.24% to 34.60%. The η, when compared to baseline, was found to be reduced for *J* of 0.192 to 0.717. For *J* 0.773 and 0.799, the η was found to be increased. The three-dimensional velocity distribution of the fluid surrounding the Model−21 grooved propeller is modified or reduced to detrimentally affect thrust. The velocity distribution along a plane bisecting the flow field along y-z for two *J* case samples, 0.334 and 0.573 is shown in Fig. 13. The results show that for *J*=0.334, the peak velocity is reduced whereas for *J*=0.573, the peak velocity is increased compared to baseline. Model − 21 produced reduced thrust for *J* from 0.192 to 0.334. From *J* of 0.383, K_T increased relative to baseline. K_P also increased relative to baseline for all *J* analyzed. The increment was found in the range of 2.24% to 34.60%. The η, when compared to baseline, was found to be reduced for *J* of 0.192 to 0.717. For *J* 0.773 and 0.799, the η was found to be increased. The three-dimensional velocity distribution of the fluid surrounding the Model−21 grooved propeller is modified or reduced to detrimentally affect thrust. The velocity distribution along a plane bisecting the flow field along y-z for two *J* case samples, 0.334 and 0.573 is shown in Fig. 13. The results show that for *J*=0.334, the peak velocity is reduced whereas for *J*=0.573, the peak velocity is increased compared to baseline. He velocity modifications in the presence of the groove modifies the pressure distribution to affect the thrust. Lower peak pressures are maintained on the pressure side (aft) as compared to baseline whereas higher low pressures are maintained on the suction side (fore) as compared to baseline for both *J*=0.334 and *J*=0.573 cases. Fig. 14 shows the modified pressure levels on the pressure side and on the suction side in the presence of groove for two *J* cases, 0.334 and 0.573 when viewed along the y-z plane bisecting the flow field.

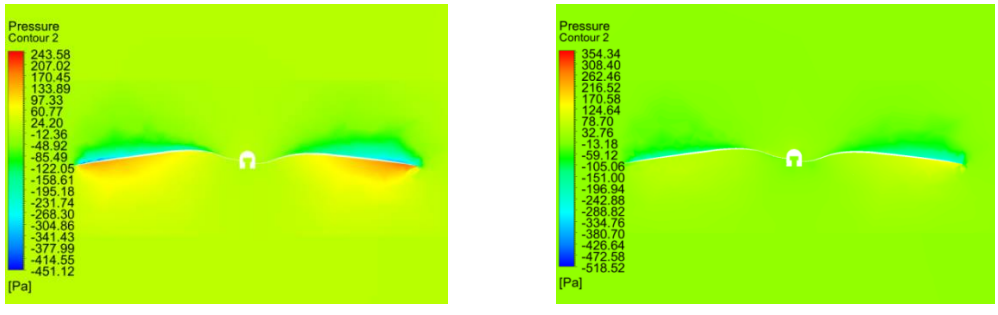

(a) (b)

Fig. 14 – Pressure contour of flow around Model − 21 propeller for (a) *J*=0.334 and (b) *J*=0.573

Vector plots of fluid flow at 0.75R radial distance and velocity distribution for three-dimensional Model−21 propeller is provided in Fig. 15 for single *J* condition *J*=0.334 to illustrate that the velocity very near to the blade surface is modified in the presence of groove.

A measure of turbulence can be provided through TKE which is a turbulence quantity. Model − 21 grooved design has increased TKE along the blade radii compared to baseline for *J*=0.334 (Fig. 16(a)) and *J*=0.573 (Fig. 16(b)).

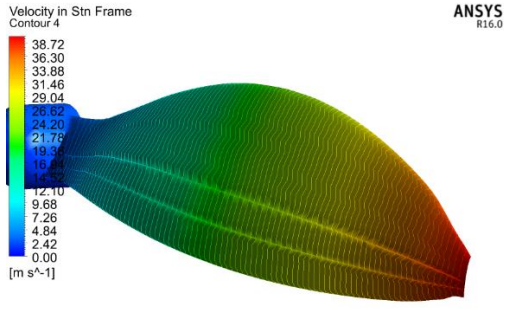

Fig. 15 – Velocity distribution on Model−21 propeller blade for *J*=0.334

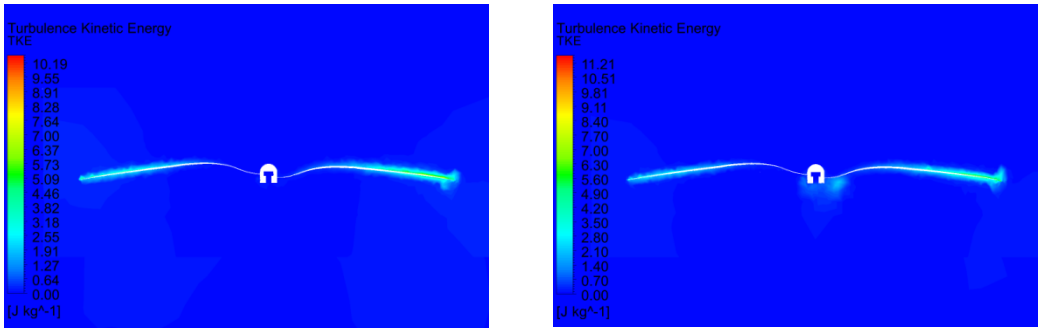

(a) (b)

Fig. 16 – Turbulence Kinetic Energy of Model − 21 propeller for (a) *J*=0.334 and (b) *J*=0.573

3.2.5 Model−22

The performance and efficiency results of Model − 22 grooved design are provided in Table 6. The relative difference between the results with baseline propeller is also listed in the table.

Model − 22 produced reduced thrust for *J* of 0.192 to 0.334. For *J* of 0.383, the thrust showed no significant improvement.

For *J* 0.432 to 0.799, the thrust was found to be increased. The increment ranged between 1.69% and 79.39%. K_P for the lowest *J* 0.192 was found to be decreased. For remaining *J*, the K_P increased relative to baseline. The η was found to be decreased for *J* of 0.192 to 0.717. For *J* 0.773 and 0.799, the η was found to be increased. The increment was found to be between 8.91% and 33.36%, respectively.

The three-dimensional velocity distribution of the fluid surrounding the Model−22 grooved propeller is modified or reduced to detrimentally affect thrust. The velocity distribution along a plane bisecting the flow field along y-z for two *J* case samples, 0.334 and 0.573 is shown in Fig. 17. It can be found that *J* change do not modify the velocity results. Comparing the results to baseline model, the peak velocity is affected or reduced for *J*=0.334. For *J*=0.573, the peak velocity remains closely similar to baseline.

Table 6 – Performance and efficiency results of Model−22

Case	Condition J	K_T	ΔK_T [%]	$10K_P$	ΔK_P [%]	η [%]	$\Delta\eta$ [%]
1	0.192	0.1160	−7.71	0.6788	−0.32	32.81	−7.58
2	0.236	0.1123	−4.89	0.6772	2.30	39.14	−7.02
3	0.282	0.1075	−3.06	0.6716	3.97	45.14	−6.73
4	0.334	0.1015	−1.13	0.6619	5.23	51.23	−6.16
5	0.383	0.0950	0.00	0.6488	6.36	56.08	−5.90
6	0.432	0.0880	1.69	0.6324	7.92	60.09	−5.96
7	0.486	0.0794	3.65	0.6089	10.11	63.37	−5.97
8	0.527	0.0723	4.52	0.5854	11.30	65.11	−6.19
9	0.573	0.0637	4.96	0.5548	12.76	65.80	−7.06
10	0.628	0.0529	7.30	0.5115	15.21	64.94	−6.83
11	0.659	0.0463	8.64	0.4845	16.19	62.95	−6.60
12	0.717	0.0336	15.77	0.4289	20.82	56.12	−4.23
13	0.773	0.0204	42.55	0.3700	30.76	42.58	8.91
14	0.799	0.0140	79.39	0.3394	34.68	32.94	33.36

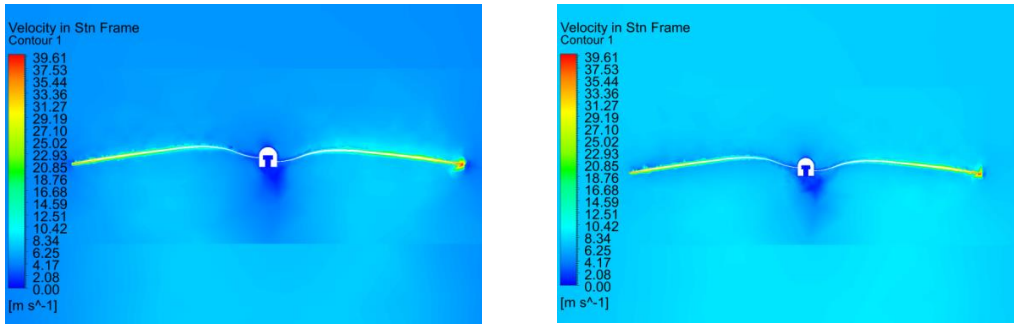

(a) (b)

Fig. 17 – Velocity flow-field around Model − 22 propeller for (a) J=0.334 and (b) J=0.573

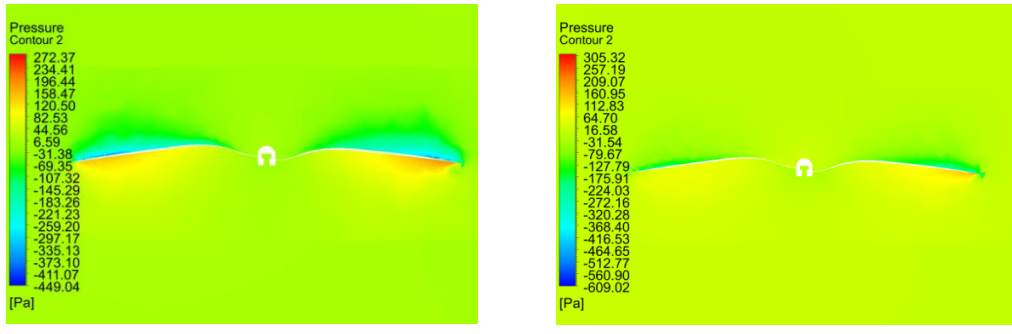

(a) (b)

Fig. 18 – Pressure contour of flow around Model − 22 propeller for (a) J=0.334 and (b) J=0.573

The velocity modifications in the presence of the groove modifies the pressure distribution to affect the thrust. Lower peak pressures are maintained on the pressure side (aft) as compared to baseline whereas higher low pressures are maintained on the suction side (fore) as compared to baseline for both J=0.334 and J=0.573 cases. Fig. 18 shows the modified pressure levels on

the pressure side and on the suction side in the presence of groove for two *J* cases, 0.334 and 0.573 when viewed along the y-z plane bisecting the flow field.

Vector plots of fluid flow at 0.75R radial distance and velocity distribution for three-dimensional Model − 22 propeller is provided in Fig. 19 for single *J* condition *J*=0.334 to illustrate that the velocity very near to the blade surface is modified in the presence of groove.

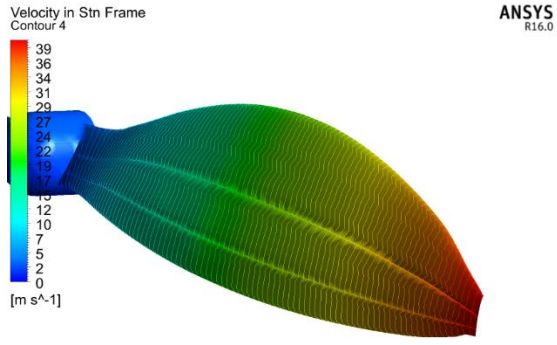

Fig. 19 – Velocity distribution on Model − 22 propeller blade for *J*=0.334

A measure of turbulence can be provided through TKE which is a turbulence quantity. Model−12 grooved design has increased TKE along the blade radii compared to baseline for *J*=0.334 (Fig. 20(a)) and *J*=0.573 (Fig. 20(b)).

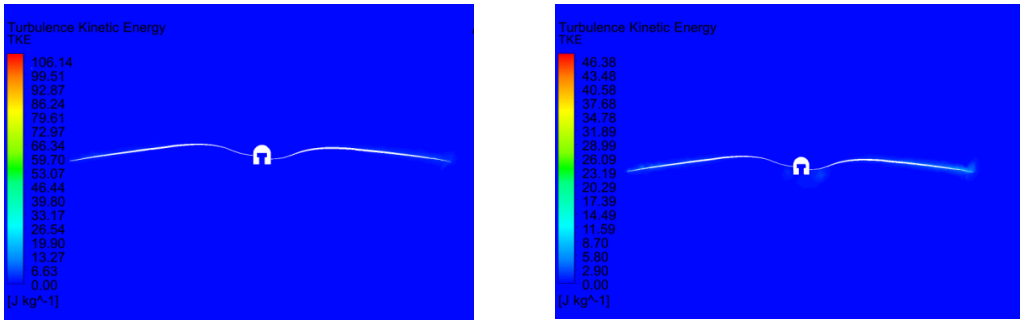

(a) (b)

Fig. 20 – Turbulence Kinetic Energy of Model − 22 propeller for (a) *J*=0.334 and (b) *J*=0.573

3.2.6 Model−23

The performance and efficiency results of Model − 23 grooved design are provided in Table 7. The relative difference between the results with baseline propeller is also listed in the table.

Model−23 produces reduced thrust for *J* from 0.192 to 0.334. For *J* from 0.383 to 0.799, K_T was found to be increased. The increase ranged between 0.36% and 77.73%. K_P was found to be reduced for *J* 0.192. From *J* 0.236, the K_P increased relatively. The η was found to be decreased for *J* from 0.192 to 0.717. For *J* 0.773 and 0.799, the η increased by 7.87% and 31.83% respectively.

The three-dimensional velocity distribution of the fluid surrounding the Model−23 grooved propeller is modified or reduced to detrimentally affect thrust. The velocity distribution along a plane bisecting the flow field along y-z for two *J* case samples, 0.334 and 0.573 is shown in Fig. 21. For this model, for *J*=0.334 case, the peak velocity is decreased compared to baseline. For *J*=0.573, the peak velocity is increased.

Table 7 – Performance and efficiency results of Model − 23

Case	Condition J	K_T	ΔK_T [%]	$10K_P$	ΔK_P [%]	η [%]	$\Delta\eta$ [%]
1	0.192	0.1159	−7.79	0.6786	−0.35	32.79	−7.62
2	0.236	0.1123	−4.91	0.6773	2.32	39.13	−7.06
3	0.282	0.1077	−2.92	0.6717	3.98	45.20	−6.62
4	0.334	0.1017	−0.94	0.6636	5.50	51.21	−6.21
5	0.383	0.0953	0.36	0.6511	6.74	56.09	−5.90
6	0.432	0.0879	1.67	0.6327	7.97	60.04	−6.04
7	0.486	0.0793	3.49	0.6082	9.98	63.35	−6.01
8	0.527	0.0724	4.59	0.5869	11.58	64.99	−6.36
9	0.573	0.0636	4.77	0.5559	13.00	65.55	−7.42
10	0.628	0.0529	7.22	0.5128	15.49	64.74	−7.12
11	0.659	0.0463	8.79	0.4866	16.68	62.77	−6.87
12	0.717	0.0336	15.89	0.4307	21.33	55.95	−4.53
13	0.773	0.0202	41.38	0.3705	30.94	42.18	7.87
14	0.799	0.0139	77.73	0.3401	34.98	32.56	31.83

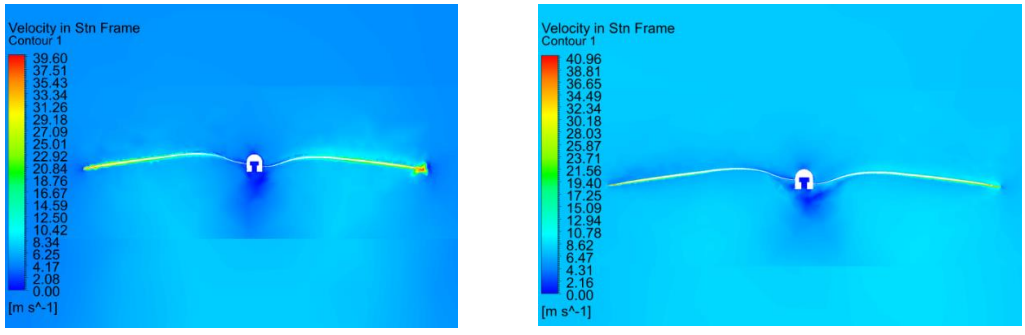

(a) (b)

Fig. 21 – Velocity flow-field around Model − 23 propeller for (a) J=0.334 and (b) J=0.573

The velocity modifications in the presence of the groove modifies the pressure distribution to affect the thrust. Lower peak pressures are maintained on the pressure side (aft) as compared to baseline whereas higher low pressures are maintained on the suction side (fore) as compared to baseline for both J=0.334 and J=0.573 cases. Fig. 22 shows the modified pressure levels on the pressure side and on the suction side in the presence of groove for two J cases, 0.334 and 0.573 when viewed along the y-z plane bisecting the flow field.

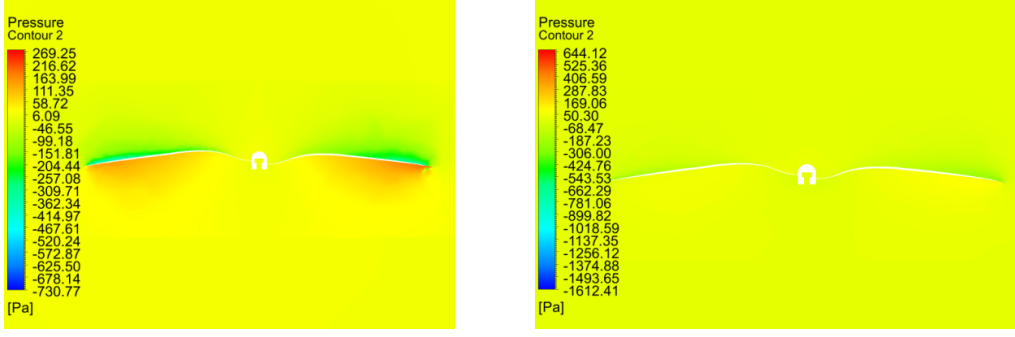

(a) (b)

Fig. 22 – Pressure contour of flow around Model − 23 propeller for (a) J=0.334 and (b) J=0.573

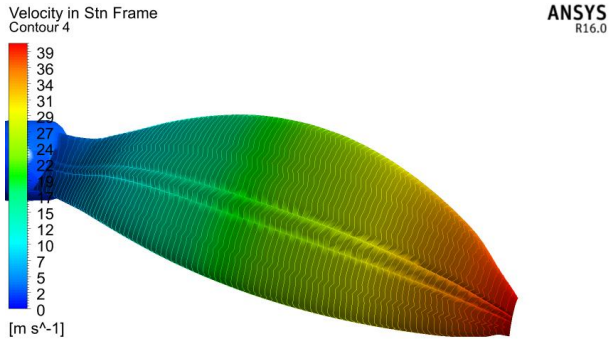

Fig. 23 – Velocity distribution on Model − 23 propeller blade for J=0.334

Vector plots of fluid flow at 0.75R radial distance and velocity distribution for three-dimensional Model − 23 propeller is provided in Fig. 23 for single J condition J=0.334 to illustrate that the velocity very near to the blade surface is modified in the presence of groove.

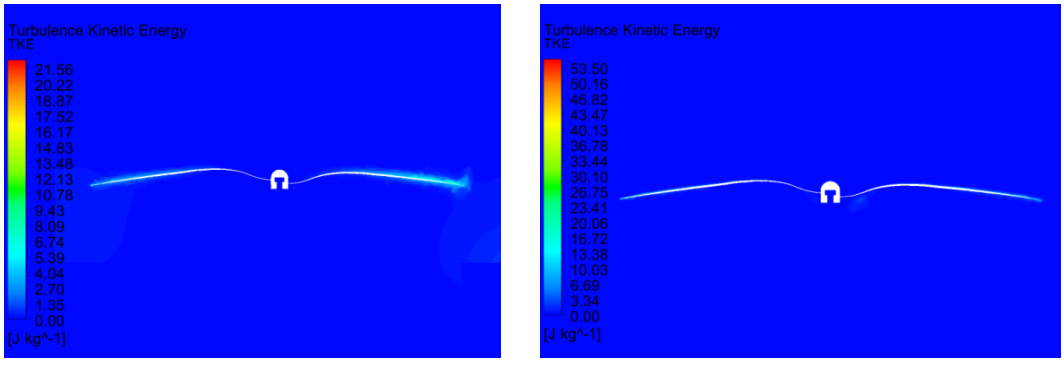

(a) (b)

Fig. 24 – Turbulence Kinetic Energy of Model − 23 propeller for (a) J=0.334 and (b) J=0.573

A measure of turbulence can be provided through TKE which is a turbulence quantity. Model−23 grooved design has increased TKE along the blade radii compared to baseline for J=0.334 (Fig. 24(a)) and J=0.573 (Fig. 24(b)).

3.3 Implication of results for UAV flight operations

Model − 18 grooved design had improved η over baseline only for one J of 0.799. Model−21, Model − 22 and Model − 23 grooved designs had improved η over baseline only for J of 0.773 and 0.799. The range of J that provides η improvement is limited. Model − 19 and Model − 20 had no η improvement over baseline for all J. Hence these models cannot be preferred over baseline design for flight operations.

4. CONCLUSIONS

Research on grooved design implemented on a UAV propeller has been completed. A CFD investigation is conducted on propellers with different groove sizes. 6 grooved designs with cross-sections of 0.1 × 0.1 mm were studied for different positions from the leading edge. The performance results revealed that in most of the 6 models, the thrust was reduced for most J between 0.192 and 0.717.

This implied that the presence of grooves modified the flow characteristics only to detrimentally impact the thrust performance. However, the grooves improved power performance due to torque reduction.

Analysis of the K_P results showed in most of the 6 models the torque reduced compared to the baseline in the low to medium J operational range. The improvement of torque, however, did not contribute to the improvement of η in all models. η is a critical parameter for propeller operation in real UAV flights.

REFERENCES

[1] A. Seeni, Effect of Groove Size on Aerodynamic Performance of a Low Reynolds Number UAV Propeller, *INCAS Bulletin*, vol. **14**, no. 1, pp. 171–186, https://doi.org/10.13111/2066-8201.2022.14.1.14, 2022.

[2] A. Seeni, Effect of Groove Size on Aerodynamic Performance of a Low Reynolds Number UAV Propeller (Part II), *INCAS Bulletin*, vol. **14**, no. 4, pp. 131-144, https://doi.org/10.13111/2066-8201.2022.14.4.11, 2022.

[3] J. Brandt, R. Deters, G. Ananda, and M. Selig, Small-Scale Propeller Performance at Low Speeds – Online Database, 2010, http://www.ae.illinois.edu/m-selig/props/propDB.html (accessed May 01, 2018).